ISSN 0965-545X, Polymer Science, Series A, 2018, Vol. 60, No. 5, pp. 594–598. © Pleiades Publishing, Ltd., 2018.

STRUCTURE AND PROPERTIES

Research on PAN Nascent Fiber Interior Microstructure through Ultrasonic Etching and Ultrathin Sectioning[1]

Quan Gao[a], Min Jing[b], Meiling Chen[a], Chengguo Wang[a,*], Shengyao Zhao[a], and Jianjie Qin[a]

[a] *Key Laboratory for Liquid–Solid Structural Evolution and Processing of Materials (Ministry of Education), Shandong University, Jinan, 250061 China*

[b] *School of Material Science and Engineering, Shandong Jianzhu University, Jinan, 250101 China*

* *e-mail: wangchg@sdu.edu.cn*

Received September 28, 2017;
Revised Manuscript Received March 31, 2018

Abstract—The interior microstructures of polyacrylonitrile nascent fibers is studied by the scanning electronic microscopy and the high-resolution transmission electron microscopy through ultrasonic etching and ultrathin sectioning. Due to the orientation and fold of molecular chains, the lamellae of 50–80 nm in thickness are formed. A high number of pores, ranging from dozens to two hundred nanometers in diameters exist between the lamellae, which result from residual solvent. The fibril structure is formed in the nascent fiber during the coagulation process, which are oriented along the fiber axis. An uneven tensile stress distribution leads to the formation of skin-core structures in the nascent fiber during the dry-jet wet spinning process.

DOI: 10.1134/S0965545X1805005X

INTRODUCTION

Polyacrylonitrile (PAN) fibers are the major precursors of the high performance carbon fibers which have an excellent potential for commercial exploitation [1, 2]. The structure and properties of PAN precursors have critical effects on the mechanical properties of final carbon fibers [3, 4]. The interior microstructure of PAN precursors, including the oriented structure, the crystal structure and the micro-voids structure is originally formed in a coagulation bath and developed during the post-treatment process of dry-jet wet spinning [5, 6]. This means that the performance of PAN precursors depends highly on the quality of nascent fibers. Therefore, it is important to understand the microstructures of nascent fibers.

A great number of earlier works were conducted to research the structures and properties of nascent fibers, mainly focusing on the cross-section, the surface morphology and the statistical structures (crystallinity, orientation and micro-pores) of the PAN nascent fiber. The characterization commonly included X-ray diffraction, nitrogen adsorption and scanning electron microscopy (SEM) and so on [7–9]. In contrast, few groups focused on the morphology of aggregation structures and stacking structures in the nascent fibers because the fiber samples suitable for electron microscopy observation are hard to be obtained.

The aggregative and the stacking structure of the fibers is usually characterized by SEM and the high-resolution transmission electron microscope (HRTEM). The fiber samples observed in SEM and HRTEM are prepared by ultrathin section method or the ultrasonic etching method [10, 11]. In this paper, the nascent fiber is treated not only by single ultrathin sectioning method or single ultrasonic etching method, but also both of them.

EXPERIMENTAL

Preparation of PAN Nascent Fiber

The PAN copolymer consisted from 99% of acrylonitirle (AN) and 1% of itaconic acid (IA) with the viscosity molecular weight $M_v = 3 \times 10^5$. The spinning dope was prepared by 17.7% copolymer and 82.3% dimethyl sulfoxide (DMSO). The dry-jet wet spinning was utilized to spin PAN nascent fiber as shown in Fig. 1. The spinning dope was extruded under the pressure through the spinneret (1000 orifices, diameter $D = 0.12$ mm) and passed through the coagulation bath (75% DMSO at 30°C). Finally, the nascent fibers were collected under the draw ratio of 5.7.

[1] The article is published in the original.

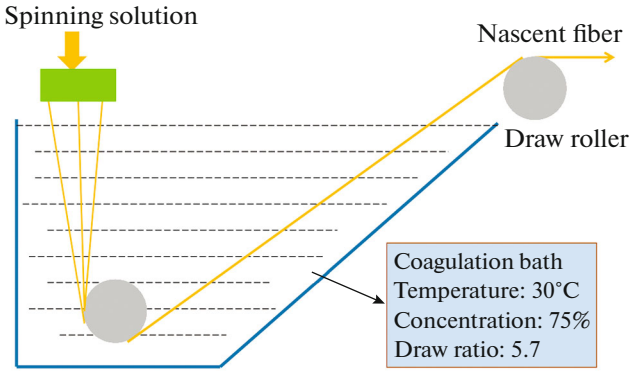

Fig. 1. (Color online) The sketch of nascent fiber coagulation process by dry-jet wet spinning.

The Sample Treatment

The principle of ultrathin section is displayed in Fig. 2. Firstly, a dozen of the nascent fibers were embedded by epoxy resin solution. In addition, the embedded block and the knife were fixed on the cantilever and the top of water sink, respectively. Then embedded block of the nascent fibers was moved downward and a slice of ultrathin section was cut. A series of ultrathin sections were obtained through reciprocating motion of block and the sections were controlled within 50 nm in thickness. Finally, the ultrathin sections were easy to float on the surface of purified water in the sink. In order to better support samples, copper grids with carbon film were used to collect ultrathin sections.

The nascent fiber was cut into 2–3 mm in length and processed ultrasonically in the 82 wt % aqueous DMSO solution at 75°C for 6h in ultrasonic cleaner. The solution was dropped on a grid and washed rapidly with distilled water of 75°C to prevent re-crystallization, then dried in the air.

The sections of nascent fiber on the grids were processed ultrasonically in 80 wt % aqueous DMSO solution at 75°C for 3 h in the ultrasonic cleaner. The section was taken out and washed rapidly with the distilled water of 75°C.

Characterization

Subsequently to coating with thin platinum layer, the microstructure of nascent fiber was observed with SEM (SU-70). The ultrathin sections were examined with HRTEM (JEM-2100).

RESULTS AND DISCUSSION

Figure 3 presents the nascent fiber morphology subsequently to solvent ultrasonic etching. Due to the dense and smooth skin, nascent fibers are partly dissolved in DMSO solution under ultrasonic treatment, its interior structure appears constantly [11]. The

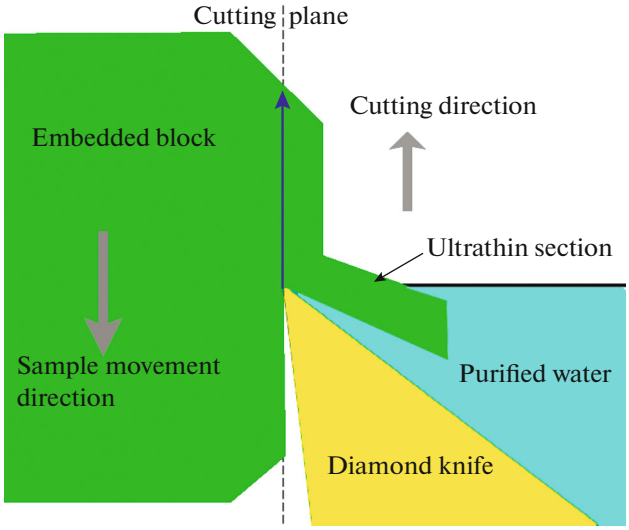

Fig. 2. (Color online) The sketch of ultrathin section process.

microfibrils are oriented along the fiber axis with diameter ranging from 70 to 170 nm. Also, grooves are formed between the fibrils because the amorphous molecular chains of the nascent fibers were etched off, which indicates that the fibrils were linked by amorphous molecular chains. The lamellae of the fibrils with 40–50 nm in thickness were perpendicular to the fibril axis.

Figure 4 presents HRTEM images of the nascent fiber longitudinal ultrathin section. As presented in Fig. 4a, a strip of fiber with 27 μm in diameter exist, in which three different areas are selected to be magnified in the skin or the core regions. In Figs. 4b–4d, the nascent fiber interior structure is composed of a great number of lamellae, which are vertically to the fiber axis in all areas, whatever in skin or in core region. However, the lamellae are packed closely and regularly with a relatively low thickness of 50 nm in the skin region, which is in conformance with the result of Fig. 3. In contrast, the lamellae are arranged loosely and in-homogeneously in the core region, being thick and high-sized of approximately 50–75 nm in thickness. The width in transverse direction ranges from tens to the hundreds nanometers. The results indicate that the lamellae are formed in the coagulation bath owing to the molecular chain folding. Also, the fold of the molecular chain proceeds on the lateral of the lamellae.

Many pores exist between the lamellae and the pores sizes range from tens to two hundred nanometers. These pores are the space occupied by DMSO solution in the nascent fibers [12]. The distribution and size of the pores could provide information of the non-solvent/solvent double diffusion during the coagulation process.

There is an apparent skin-core structure existed in Figs. 4b and 4d, where the skin width was approxi-

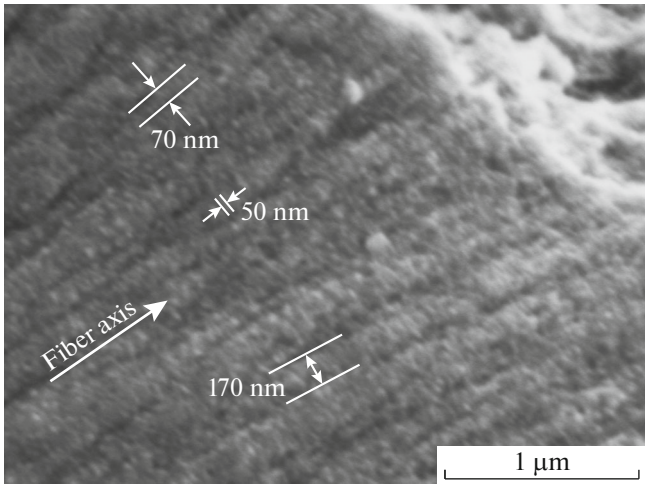

Fig. 3. SEM image of nascent fiber following solvent etching.

mately 500 nm. The skin-core structure in the longitudinal sections results from the degressive strain distribution during the coagulation bath. A higher tensile stress is applied on the fiber surface and the tensile stress gradually drops down at the center of the fiber. The tensile stress difference in the transverse direction leads to the lower thickness and closer arrangement of the lamellae in the skin region, compared to the center of the nascent fiber. Eventually, the skin-core structure of the nascent fiber forms.

Figure 5 presents HRTEM image of nascent fibers longitudinal ultrathin section following ultrasonic etching. As is shown on Fig. 5a, the partial nascent fiber section has already been dissolved, where the pores and cracks form due to removal of the amorphous structures. Figure 5b presents nascent fiber surface magnified image in Fig. 5a. The lamellae are destroyed, then the microfibril structures appear after the ultrasonic etching treatment, indicating the existence of the fibrils structures. Only when the structures are separated, the arrangement of longitudinal microfibrils could be demonstrated [11].

The microfibrils, in-between 26–40 nm in diameter, were oriented along the fiber axis and arranged closely. Figure 5c displays the morphology of the core of the nascent fiber. The microfibrils, with the relatively low diameter of 21–30 nm, were loosely arranged. The results provide the direct evidence for the existence of the fibril structure in the nascent fiber

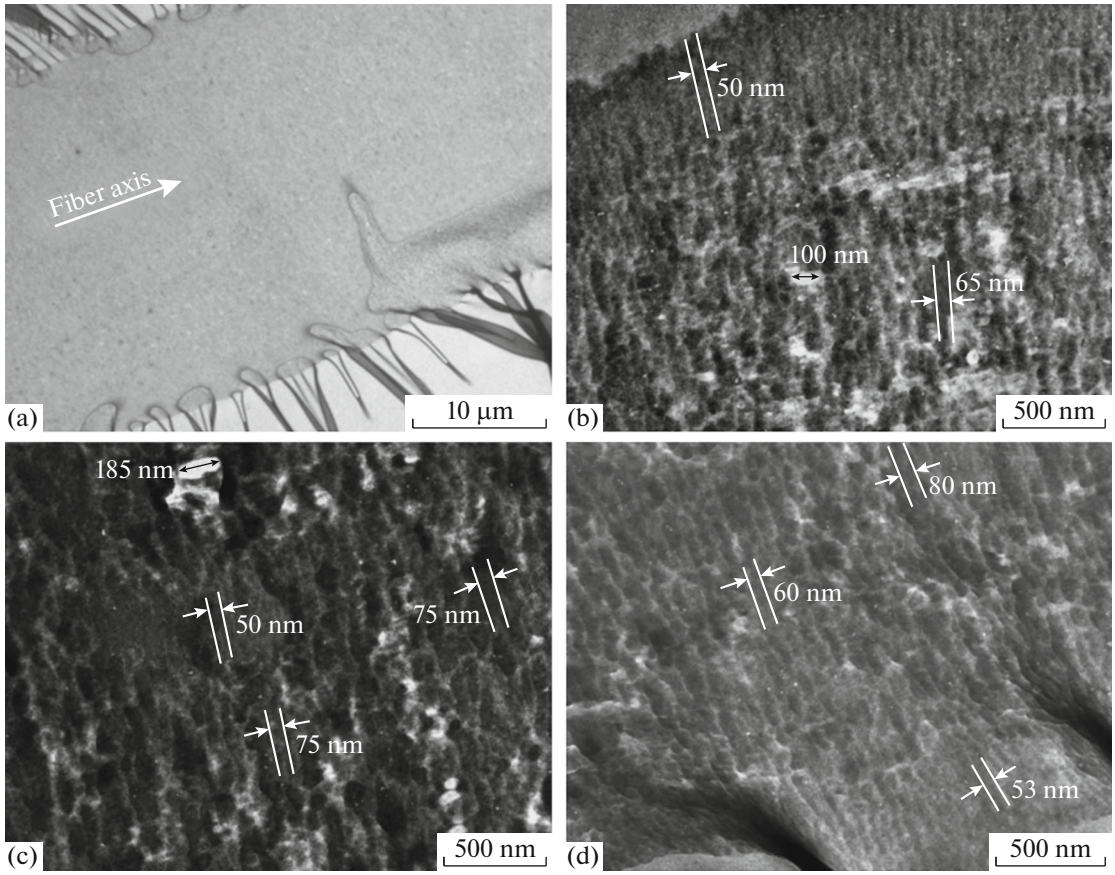

Fig. 4. HRTEM images of nascent fiber longitudinal ultrathin section. (a) Low magnification image; (b, c, d) high magnification image.

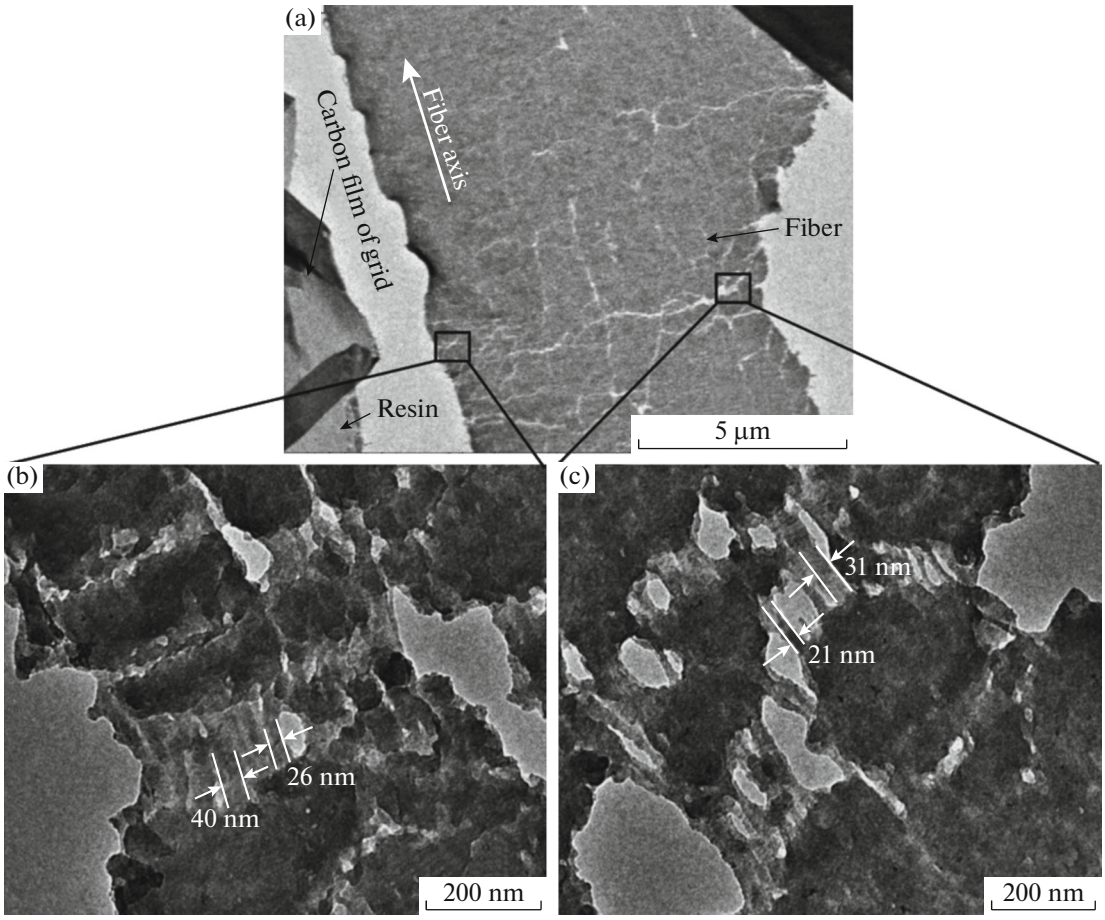

Fig. 5. HRTEM images of nascent fiber longitudinal ultrathin section following ultrasonic solvent etching. (a) Low magnification image; (b, c) high magnification image.

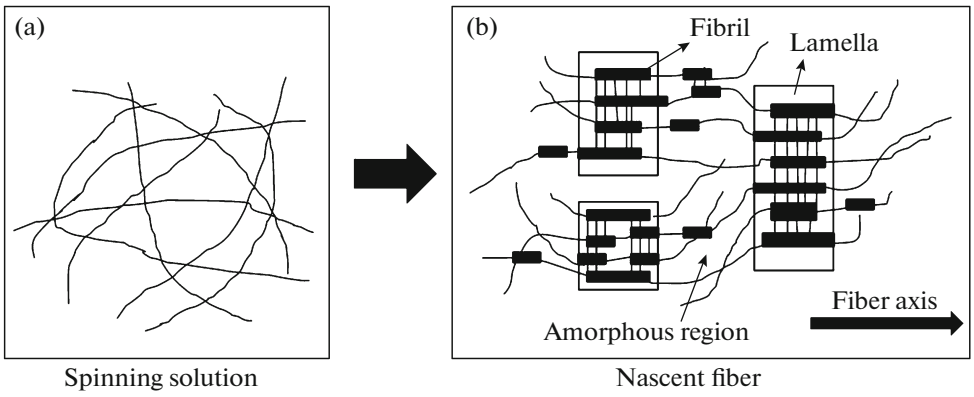

Fig. 6. Schematics of the molecular chain during coagulation transition: (a) spinning dope; (b) nascent fiber.

and demonstrate that the fibril structures form in the coagulation bath stage.

The scheme in Fig. 6 depicts the transition of molecular chain during coagulation. Figure 6a displays the random distribution of PAN molecular chain in the spinning dope. When the spinning dope passes through the spinneret under drawing stress in coagulation bath, the molecular chains are folded and oriented, then the fibrils are formed. Certain microfibrils are linked by amorphous molecular, which lead to the formation of the lamellae, as presented in Fig. 6b. A single molecular chain might go through several

lamellae. The microstructural transformation during coagulation process is accomplished by chain slipping within lamellae, which could be attributed to the arrangement and orientation of the microfibrils, promoting the preparation of highly quality PAN precursors.

CONCLUSIONS

The interior microstructures in the nascent fibers were obtained in SEM and HRTEM through the ultrasonic etching and ultrathin sectioning methods. During the coagulation process, the PAN molecular chains are oriented and folded, to form the lamellae and fibril structures. Many pores exist within the PAN nascent fibers longitudinal ultrathin section owing to the residual DMSO solvents. The formation of skin-core structures in the nascent fiber could be ascribed to an uneven tensile stress distribution. These results do not only display the interior microstructure within the nascent fiber, whereas also provide certain information control probability for nascent fiber microstructure. They are good to prepare the excellent PAN precursor and ultimately the high performance carbon fiber.

ACKNOWLEDGMENTS

This work was supported by the National Natural Science Foundation (Grant nos. 51773110 and 51573087) and Technology Project of Shandong Province (Grant no. J14LA05) of China.

REFERENCES

1. L. Tan, A. Wan, and D. Pan, Mater. Lett. **65**(5), 887 (2011).
2. X. Guo, Y. Cheng, Z. Fan, Z. Feng, L. L. He, R. Liu, and J. Xu, Carbon **109**, 444 (2016).
3. X. Liu, C. Zhu, J. Guo, Q. Liu, H. Dong, Y. Gu, R. Liu, N. Zhao, Z. Zhang, and J. Xu, Mater. Lett. **128** (6), 417 (2014).
4. W. Zhang, L. Jie, and W. Gang, Carbon **41** (14), 2805 (2003).
5. L. Tan, H. Chen, D. Pan, and N. Pan, J. Appl. Polym. Sci. **110** (4), 1997 (2008).
6. X. Zeng, J. Chen, J. Zhao, C. Wu, D. Pan, and N. Pan, J. Appl. Polym. Sci. **114** (6), 3621 (2010).
7. Y. X. Wang, C. G. Wang, and M. J. Yu, J. Appl. Polym. Sci. **104** (6), 3723 (2010).
8. A. F. Ismail, M. A. Rahman, and A. Mustafa, Chem. Mater. **18** (12), 4465 (2006).
9. X. Dong, C. Wang, J. Chen, and W. Cao, J. Polym. Res. **15** (15), 125 (2008).
10. Q. Wang, C. Wang, M. Yu, J. Ma, X. Hu, and B. Zhu, Sci. China: Technol. Sci. **53** (6), 1489 (2010).
11. Q. Wang, C. Wang, Y. Bai, M. Yu, Y. Wang, B. Zhu, M. Jing, J. Ma, X. Hu, and Y. Zhao, J. Appl. Polym. Sci. **48**, 617 (2010).
12. J. Hao, C. Lu, P. Zhou, and D. Li, Thermochim. Acta **569**, 42 (2013).